# Effect of Tunneling on Shallow Foundations

* El Naggar, Abdelmoneim [1] Youssef, Maged A. [2] El Naggar, Hany [3]

[1], [2] *Civil and Environmental Engineering, Western University, London, ON, Canada*
[3] *Civil and Resource Engineering, Dalhousie University, Halifax, NS, Canada*

[1] aelnagg3@uwo.ca
[2] youssef@uwo.ca
[3] hany.elnaggar@dal.ca

## ABSTRACT

Effect of tunneling on nearby structures must be assessed to eliminate the potential for structural failures. Such assessment requires a deep understanding of the soil-structure interaction (SSI) of buried and surface structures. This paper focuses on structures supported by shallow foundations and provides an assessment of the available numerical and finite element analysis techniques. The assessment is made based on the ability to capture: (1) the complicated nonlinear behavior of the soil and the tunnel, (2) the effect of surface settlement, (3) the development of earth pressure along the tunnel lining, and (4) the construction sequence. The paper also discusses the limitations and accuracy of the considered methods.

## 1. INTRODUCTION

Population growth is one of the greatest burdens for many countries. Many megacities cannot support the influx of human demand on its infrastructure. For example, the demand on the USA transportation infrastructure costs the average person 54 hours of wasted time a year because of traffic congestions. This cost increases for major cities such as Los Angeles, where it reaches 119 hours (Elis and Glover, 2019). The great shift to urbanization only adds to this problem. Currently, over 84% of North America's population lives in urban areas. Likewise, any population increase within North America is more likely to affect these overly saturated metropolitan spaces directly. The only viable infrastructure solution to this problem is to rely more on underground

---

[1] Graduate Student
[2] Professor
[3] Professor

transportation systems, which requires constructing underground tunnels in heavily populated areas.

Tunnel excavation inevitably results in ground movements, which affect the foundations of the neighboring surface structures. If the effects of such movements are not carefully examined, adjacent structures could deform, distort, or develop irreparable damage (Zhang et al. 2013 & Zakhem and El Naggar 2020). Such damage would result in financial losses, along with serious social impacts. Ground movements should not only be assessed during construction but also during the service life of the tunnel.

This paper provides a comprehensive literature review for available modeling techniques to anticipate ground movements during and after the construction of underground tunnels. It provides the necessary knowledge for tunneling engineers to account for such movements. The paper starts with a brief description of current methods to construct underground tunnels and potential effects on shallow foundation systems. The paper then presents a detailed review of available modeling techniques.

## 2. Construction of Underground Tunnels

Tunnel excavation is commonly conducted using closed shield tunnel boring machines (TBMs) or Earth pressure balance machines (EPB). TBMs are most widely used, as they can deal with any soil condition, regardless of groundwater level (Zakhem and El Naggar, 2019). They have facilitated the evolution of rapid excavation by shield driven methods, in which precast segmental concrete tunnel linings are used. Shield driven tunneling permits a single pass installation, eliminating the need for a secondary tunnel support system, which is required by other methods such as the New Austrian tunneling method (NATM). The boring machine remains stationary during the construction of each segment. This fast installation ability minimizes ground movements (El Naggar, 2007).

TBMs offer a stable tunnel excavation procedure, as the process involves mixing the excavated soil with slurry to get pumped back under pressure and help stabilize the working face, thereby preventing collapse by balancing the surrounding earth pressures in the ground. Hence, such stabilizing factors, and the ability to control groundwater and minimize the surrounding ground movements, while maintaining cost-effectiveness, make TBM very common in the tunnel excavating industry.

## 3. Effect of Tunneling on Shallow Foundations

The tunnel excavation procedure involves removing large volumes of underground geomaterials, which results in the relaxation of in-situ stresses within the vicinity of the tunnel and makes displacement and local deformation inevitable. The changing stresses within the vicinity of the tunnel directly affect the ground deformation, as the geomaterial around the opening starts to move. Even though tunnel linings are placed to reduce such movement, it is very difficult to perfectly fit the lining instantly at the excavation opening, resulting in some ground deformation, commonly known as the tunneling gap (El Naggar et al. 2008). In certain cases, the consolidation, soil creep and porewater pressure

diffusion would occur, resulting in an increased ground movement over time. Such displacements propagate outwards from the excavation opening, eventually accumulating at the top surface of the soil, resulting in what is known as surface settlement (Negro and Queiroz, 2000; Ongsuksun, 2009).

Ground movements propagating outwards from excavated tunnel openings would result in vertical and horizontal ground displacements. When such displacements reach the top-soil layer, settlement troughs are created. These surface troughs result from the stress relief in the affected zone. Combining them with the developed horizontal strains could result in damaging the surrounding structures (Schmidt, 1969). Damage examples, associated with the tunnelling process near Cerrahpaşa Medical Faculty, Istanbul, Turkey, are shown in Figure 1 (Yildizlar et al., 2014).

(a)

(b)

**Figure 1:** Damage due to ground movement (a) Non-structural damage; (b) Structural damage

## 4. Modelling Techniques

The modelling of shield driven tunnels must consider the effects of the soil nonlinearity and the other complications that could arise from the excavation sequence. Also, certain

design parameters, which are based on the soil structure interaction, would need to be determined to effectively assess the effect of tunnelling on the surrounding structures. Aspects that would need to be considered in such assessment would include the interaction between the TBM machine and the surrounding ground, the applied face pressures, and shear transfer between the ground interface and the tunnel lining. The face pressures are required to maintain equilibrium between the developed stresses, the earth pressure, and the machine chamber pressure. Face stability is also needed to prevent the uncontrolled flow of soil. The segmental tunnel lining, the jacking forces, and the tail void grouting and injection pressure are also important aspects that could be included to improve the modelling results. Modelling efforts differ in their complexity, which results in different predictions. The two main methods for assessing the effects of tunneling on building performance are given in the following subsections.

### 4.1 Uncoupled Soil-Structure Interaction Methods

In uncoupled soil structure interaction methods, analysis is divided into two stages. In the first stage, the ground movement at free-field conditions, ignoring the nearby structures, is assessed. The second stage involves imposing the derived movements from the first stage on the modelled structures to evaluate their performance. A summary of the empirical, analytical, and numerical methods used in the first stage of analysis is given below.

#### 4.1.1 Empirical Methods

The earliest methods developed to describe ground settlement due to tunneling were simply based on concepts arising from observations collected during mining. In 1913, after observing settlements patterns above coal mines in Europe, Goldreich proposed Equation 1 to evaluate the maximum settlement.

$$\frac{s'_{max}}{t} = 1 - \kappa\frac{z_0}{t}; \qquad where\ \kappa = \frac{V_o - V_s}{V} \qquad \text{Equation 1}$$

Where $\kappa$ is an empirical coefficient of expansion that ranges between 0.01 and 0.03, $V$ is the volume of the subsiding body, $V_o$ is the excavated volume, and $V_s$ is the volume of the settlement trough.

In 1929, Briggs developed Equation 2, which assumed the ratio $\frac{S'_{max}}{t}$ to be solely dependent on the depth of the excavated tunnel.

$$\frac{S'_{max}}{t} = \frac{1}{1+0.045\sqrt{z_o}} \qquad \text{Equation 2}$$

Where $S'_{max}$ is the maximum settlement possible within the subsidence trough pattern, t is the thickness of the mined seam, and $z_o$ is the depth (in meters).

Both equations 1 and 2 establish that the ratio $\frac{S'_{max}}{t}$ is independent of the width of the opening, and that it decreases with the increase of the depth of the subsiding body.

These equations, however, are only valid for wide supercritical profiles. Furthermore, they are not accurate for tunnels in soft ground.

After analyzing subsidence troughs, Martos (1958) modeled the relationship between the transverse distance from the tunnel's centerline (y) and the surface settlement using Gaussian distribution, Equation 3. This relationship was defined based on statistical evaluation of settlements above the Hungarian tabular mine openings.

$$\frac{S}{S_{\max}} = e^{x^2/2i^2} \qquad \text{Equation 3}$$

Where S stands for surface settlement at a transverse distance y from the tunnel's centerline, $S_{max}$ is the maximum settlement possible at a given transverse distance from the centerline of the tunnel, $x$ is the horizontal distance, and $i$ is the curve's standard deviation corresponding to the y value of the curve at the point of inflection.

Another well-known empirical method is the Peck-Fujita method, which is similar to Martos (1958) relationship. This Gaussian distribution function, Equation 4, was developed by Peck (1969) based on field data.

$$S_{(x)} = S_{max} exp\left(\frac{-x^2}{2i^2}\right) \qquad \text{Equation 4}$$

Based on 94 settlement cases in Japan, Fujita (1982) statistically analyzed the maximum surface settlement caused by shield tunneling. Figure 2 shows the comparison of the developed Peck-Fujita method predictions and the data collected from a 1.5 m wide tunnel with a centerline depth of 6.5 m, which was driven with a hand-excavated open shield through a clayey soil at the Haycroft relief sewer (Glossop and O'Reilly, 1982).

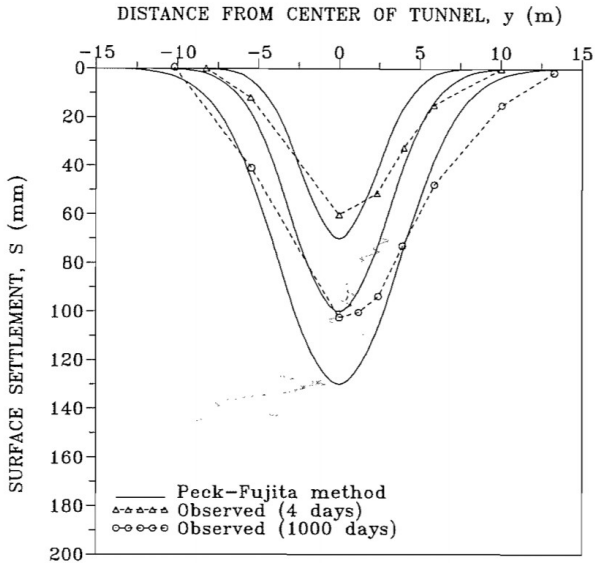


**Figure 2:** Accuracy of Peck-Fujita method predictions (Fang et al., 1994; redrawn from Glossop and O'Reilly, 1982)

Terzaghi (1942) developed a parabolic subsidence profile based on observations from the Chicago subway tunnels. Trough width, depth, and tunnel radius were found to be proportionally related to each other as per Equation 5. The volume of ground loss $V_s$ can be described by Equation 6.

$$w = 1.4a + z_o \qquad \text{Equation 5}$$

Where $w$ is the trough width, $a$ is the excavated tunnel's radius, and $z_o$ is the depth to the tunnel axis.

$$V_s = \frac{2}{3} S_{max}(1.4a + 0.6z_o) \qquad \text{Equation 6}$$

Terzaghi established that the ratio of maximum ground settlement to trough width should not be taken less than 0.005 within built-up areas.

Another simple subsidence curve was developed in the form of a triangular profile to describe the relationship between the maximum settlement produced and the volume of the ground lost (Mandel and Wagner 1968), as described in Equation 7. Even though the triangle profile does not accurately depict the actual gaussian bell shape of the ground subsidence, it effectively predicts the maximum settlement point, occurring at the center of the profile, as shown in Figure 3.

$$S_{max} = \frac{V_s}{0.58(a+z_0)} \qquad \text{Equation 7}$$

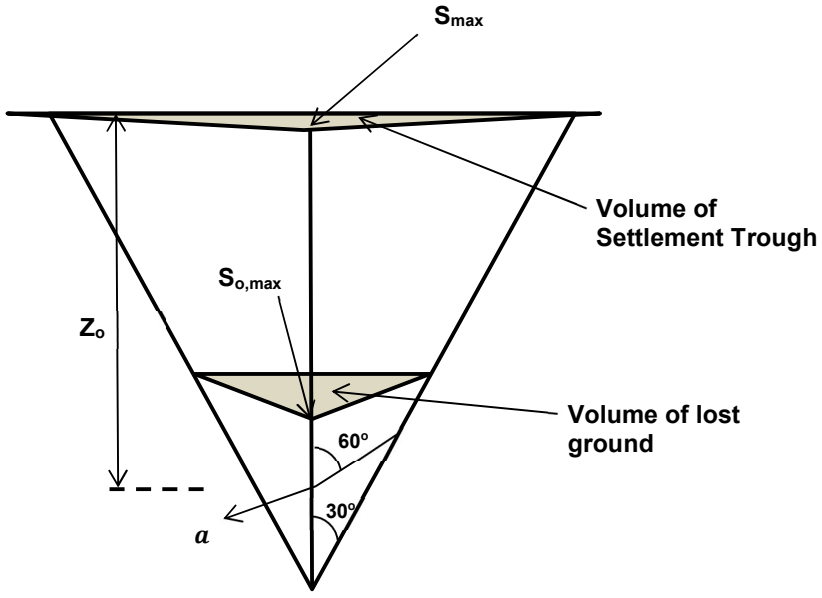


**Figure 3:** The developed triangular subsidence profile (After Terzaghi, 1942)

Likewise, Schmidt (1969) considered the subsidence and other movements generated by tunneling in a variety of geologic media, including rock mediums, with primary concern on single and twin shallow tunnels that can be excavated without blasting or rock cutters. A reliable relationship, Equation 8, to predict the width and geometry of the subsidence trough while incorporating the influence of the construction process via field experience was developed. The shape and width of the subsidence trough were found to be nearly independent of the subsidence magnitude, but dependent on the geometry.

$$S_{max_{(z)}} = S_{max_{(0)}} \left(\frac{z_o}{z_o - z}\right)^{0.8} \quad \text{Equation 8}$$

Where $S_{max_{(z)}}$ is the maximum subsidence at depth $z$, $S_{max_{(0)}}$ is the maximum subsidence at the ground surface, and $z_o$ is the depth to the tunnel axis.

O'Reilly and New (1982) developed equation 9 to estimate subsidence and validated the equation using data from several sites. This equation, however, is not applicable in the region within the diameter of the tunnel periphery.

$$S_{max_{(z)}} = \frac{V_s}{\sqrt{2\pi}K_z} \exp - \frac{y^2}{2(K_z)^2} \quad \text{Equation 9}$$

Where K is an empirical constant of proportionality, z is the height above the tunnel's axis, y is the transverse distance from the centerline, and $V_s$ is the settlement volume.

### 4.1.2 Analytical Methods

Verruijt and Booker (1996) presented a useful solution for displacements and stresses around excavated tunnels at moderate depth in an elastic soil medium. The tunnel undergoes a relatively small ovalization resulting in wider surface transversal settlement troughs. This ovalization, along with radial displacement, was considered as an input parameter in their proposed solution described by Equation 10. This closed-form solution could be used for any value of Poisson's ratio and at any point in the soil. However, it should be noted that it is based on the assumption of incompressible soil behaviour (i.e., not suitable for medium and soft soils).

$$s_{max} = -\varepsilon R^2\left(\frac{z_1}{r_1^2} + \frac{z_2}{r_2^2}\right) + \delta R^2\left[\frac{z_1(kx^2 - z_2^2)}{r_1^4} + \frac{z_2(kx^2 - z_2^2)}{r_2^4}\right] + \frac{2\varepsilon R^2}{m}\left[\frac{(m+1)z_2}{r_2^2} + \frac{mz(x^2 - z_2^2)}{r_2^4}\right] - 2\delta R^2 h\left[\frac{x^2 - z_2^2}{r_2^4} + \frac{m}{m+1}\frac{2zz_2(3x^2 - z_2^2)}{r_2^6}\right] \quad \text{Equation 10}$$

Where $z_1 = z - H$, $z_2 = z + H, r_1^2 = x^2 + z_1^2$, $r_2^2 = x^2 + z_2^2$, $m = \frac{1}{1-2v}$, $k = v(1-v)$, $\varepsilon$ is the uniform radial ground loss, $s_{max}$ is the long term ground deformation due to the ovalization of the tunnel lining, R is the tunnel radius, H is the tunnel depth, and $v$ is the soil's Poisson's ratio.

Loganathan and Poulos (1998) modified Verruijt and Booker (1996)'s solution and redefined the ground loss based on the gap parameter (g) as given by Equation 11 and shown in Figure 4. Gap parameter is the magnitude of the equivalent two-dimensional void formed around the tunnel due to the effects of the three-dimensional elastoplastic ground deformation at the tunnel face $(U^*_{3D})$, excavation of soil around the tunnel shield's circumference, quality of workmanship $(\omega)$, the tunnelling machine physical gap $(G_p)$, and the lining geometry (Rowe and Kack, 1983).

$$g = G_p + U^*_{3D} + \omega$$ Equation 11

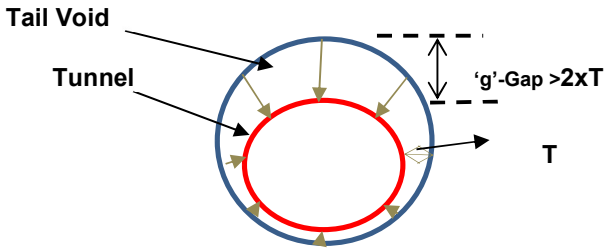


**Figure 4:** Oval-shaped ground deformation pattern around the tunnel section (After Loganathan and Poulos,1998)

The ground loss parameter greatly influences the ground deformation pattern, which occurs in two stages: loss in the undrained state and due to ground consolidation and creep. Equation 11 predicts the surface settlements above the centerline. Its predictions were compared to five different case studies, and Good agreement has been observed for subsurface settlements and horizontal movements for uniform clay profiles. Figure 5, modified after Verruijt and Booker (1996), shows a comparison between the predicted and actual settlement for Heathrow Express Trial Tunnel.

$$s_{max} = R^2\{-\frac{z-H}{x^2+(z-H)^2} + (3-4\nu)\frac{z+H}{x^2+(z+H)^2} - \frac{2z[x^2-(z+H)^2]}{[x^2+(z+H)^2]^2}\}\frac{4Rg+g^2}{4R^2}\exp\{-[\frac{1.38x^2}{(H+R)^2} + \frac{0.69z^2}{H^2}]\}$$

Equation 11

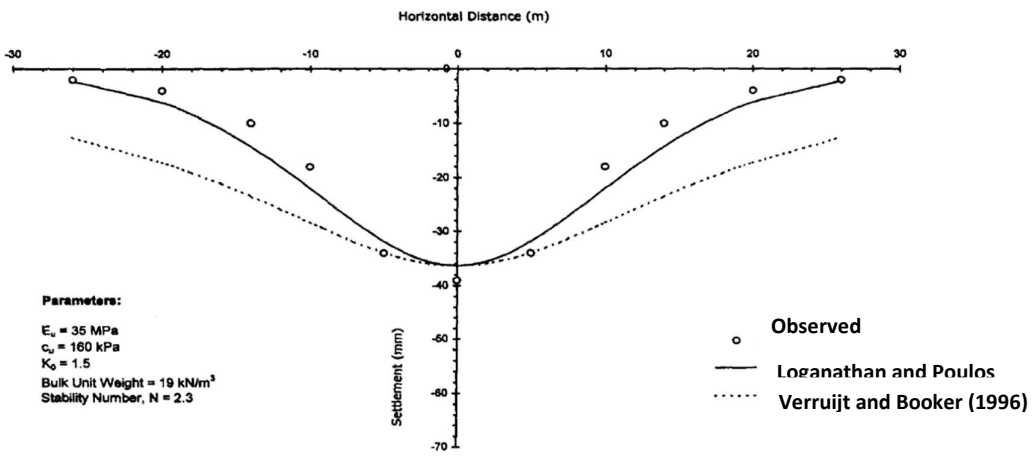

**Figure 5:** Observed and predicted surface settlement for Heathrow Express Trial Tunnel

Einstein and Schwartz (1979) utilized the relative stiffness method to develop a simplified analytical solution, Figure 6, that models the effects of the most significant ground and support characteristics to aid in tunnel design. To develop this simplified model, first they derived the initial displacement field in ground mass due to in-situ stresses. Then the stresses in the ground mass were expressed in terms of Mitchel's generalized stress function. The stress and incremental displacement fields in the ground after excavation and contact stresses at ground support interface effects were determined. Equation 12 corresponds to the combined ground movements from both initial ground stresses and stress redistribution induced by the excavated circular opening.

$$s_{max} = \frac{1+v}{E}\{-a_o r^{-1} + \frac{1}{2}\mathrm{Pr}\,(1+K) - \frac{1}{2}\mathrm{Pr}\,(1-K)\cos\,2\theta + \sum_{n=2,4,6}^{\infty}[na'_n r^{-n-1} + (n+2)b'_n r^{-n+1}]\cos\,(n\theta)$$ Equation 12

Where K is the ratio of lateral to vertical stress (k=0 to 4), v is the ground mass' Poisson's ratio, E is the elastic modulus, P is the initial vertical stress, and $\theta$ is the angle measured counter-clockwise from the tunnel spring line.

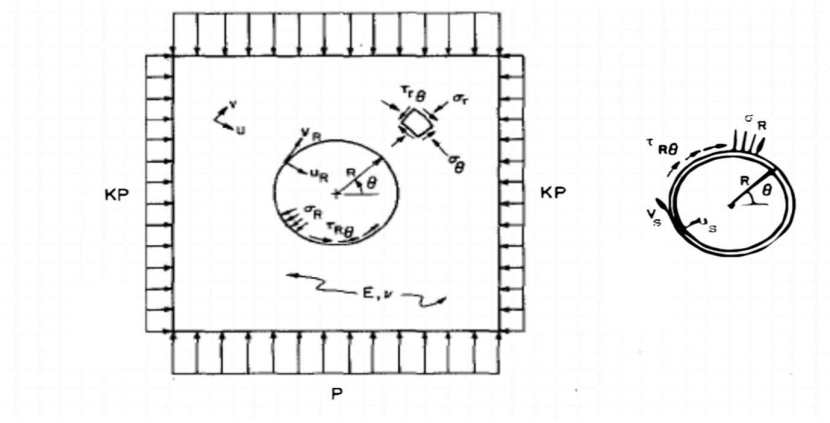


**Figure 6:** Einstein and Schwartz (1979)'s depiction of the tunnel

Movements due to initial ground stresses occurs before the tunnel is excavated, and does not directly affect the ground support interaction. Hence the initial ground displacements due to the existing in-situ stresses were subtracted from the combined ground movements due to the initial ground stresses and the stress redistribution. This leads to Equation 13, which is an incremental displacement equation describing the excavation unloading condition for tunnels.

$$s_{max} = \frac{1+v}{E}\{-a_o r^{-1} + \sum_{n=2,4,6}^{\infty}[na'_n r^{-n-1} + (n+2-4v)b'_n r^{-n+1}]\cos\,(n\theta)\}$$ Equation 13

Bobet (2001) expanded the work of Einstein and Schwartz (1979) along with other researchers ( Bouvard and Pinto, 1969; Bobet, 2001; Matsumoto and Nishioka, 1991);

Fernandez et al., 1994)) by developing analytical solution considering a shallow tunnel in both dry and saturated conditions. The ground and liner were assumed to be fully elastic, which restricts the developed solution to ground conditions where the deformations are small (stiff clays and rocks), or when the excavation method prevents large ground deformations (shield excavation methods). The solution takes into account the effect of the different construction processes by analyzing the effect of air pressure and the gap between the tunnel concrete liner and the surrounding ground. This solution, however, does not account for behavior of ground or liners with time such as swelling and creep. Full slippage between the ground and liner was assumed, due to the small coefficient of friction present. The solution describing the maximum ground settlement in dry ground conditions is given by Equation 14.

$$s_{max} = -\frac{wr_a}{H} + \frac{1+v}{E}\left\{\gamma r_c^2 \left| \begin{array}{c} \frac{1}{8}\left(k - \frac{v}{1-v}\right)\left(\frac{r_a}{H}\right) - \frac{1}{4}\frac{3-4v}{1-v}\ln H \\ +\gamma H(1-k) r_n \left[-2(1-v)\frac{r_0}{h} + \frac{1}{8}(9-4v)\left(\frac{r_o}{H}\right)^3 - \frac{1}{4}\left(\frac{r_g}{H}\right)^s\right] \end{array} \right.\right\}$$

Equation 14a

$$w = \frac{ground\ loss\ (\%)}{200} * r_o$$

Equation 14b

Where $w$ is the magnitude of the gap between the tail of the shield and the liner, $r_o$ is the circular cross sectional radius, $E$ is the soil elastic modulus, $v$ is the soil's Poisson's ratio.

Similarly, Bobet (2001) developed two forms of the solution for both short term analysis and long-term analysis. Short term analysis refers to the conditions where excavation and liner installation in a saturated ground are assumed to occur rapidly as compared to the ground permeability, thereby preventing the formation of excess pore pressure. Unlike dry ground where the stresses are constant, short term construction and saturated ground yield greater stresses. The complete short-term solution is obtained through the superposition of saturated ground without water pressure and the solution considering water pressure only. The solution showed that the presence of water increases the loads on the liner but decreases the settlements at the surface, due to the reduction of the ground unit weight from the total weight to buoyant weight. Long term analysis refers to the condition where a long time has elapsed after construction, and the excess pore pressure dissipates. The complete solution for long term analysis is obtained by summing the saturated ground without water pressure solution and either the water pressure and no drainage solution only or the water pressure and drainage solution.

### 4.1.3 Numerical Methods

Numerical simulations can provide practical assessments of the performance of a given tunnel (Zakhem and El Naggar, 2019). Two-dimensional numerical simulations are mostly used for uncoupled modeling efforts. Amorosi et al. (2012) developed a 2D numerical simulation of a 10 m wide tunnel located 20 m under a masonry wall utilizing the finite element program Abaqus. The soil mesh was composed of 8-node quadrangular plane strain elements. The tunnel excavation process was simulated by

de-activating the soil elements inside the tunnel section and replacing them with equivalent nodal forces at the tunnel boundaries and gradually reducing these forces to simulate the tunnel face advancement. Figure 7 shows the deformed mesh under different percentages of unloading in free field analysis. This free-field numerical analysis showed that increasing the percentage of nodal forces unloading leads to a progressive deepening of the subsidence profile. Also, the tunnel section deforms into an ellipse characterized by a maximum horizontal axis, as shown in the figure. These deformations and settlements are then applied to the wall being analyzed to determine the expected behavior under such conditions.

### 4.2 Coupled Soil-Structure Interaction Methods

In coupled soil structure interaction, the ground strata, tunneling process, and nearby structures can all be modelled using two- or three-dimensional numerical methods.

#### 4.2.1 Two-Dimensional Methods

Even though two-dimensional methods are best suited for free field conditions, it is one of the most common numerical simulations. It can be conducted with the use of finite element software such as PLAXIS, Abaqus, and others. Amorosi et al. (2012) realized that coupled soil-structure analysis enhanced the accuracy of the excavation induced settlements. It requires the utilization of suitable constitutive models for the soil, lining material, and their interface.

When developing 2D numerical simulations, tunnel boundary progressive displacements must be recreated, so that the progressive development of loads and displacements are captured. To include some of these 3D effects in 2D numerical simulations, 2D modelling procedures may adopt any of the following techniques (Karakus, 2006): Straight excavation, Average pressure reduction, Excavation of concentric rings, and Face de-stressing. The straight excavation modeling technique involves excavating the defined material, allowing the determination of instantaneous displacements. It is used to model excavations occurring in hard homogeneous rock masses. Certain aspects, like the 3D plasticity effects, pre-convergence, and stress distributions, are compromised in this modelling technique. Average pressure reduction involves the application of an internal pressure equal to the initial in situ stresses. This pressure is then gradually decreased until reaching a zero normal stress, mimicking the gradual loss of resistance arising from the excavation process. This method is used to provide a preliminary assessment of the support requirements for circular tunnels. Excavation of concentric rings involves excavating the tunnel in stages from the center of the desired tunnel, where the central region represents the weakening of the material ahead, while the outer rings represent the open cavity. Face destressing involves the gradual replacement of the tunnel core with unstressed elastic material. The tunnel core can provide coverage until temporary stress equilibrium is reached (Vlachopoulos and Diederich, 2014).

FREE-FIELD ANALYSIS

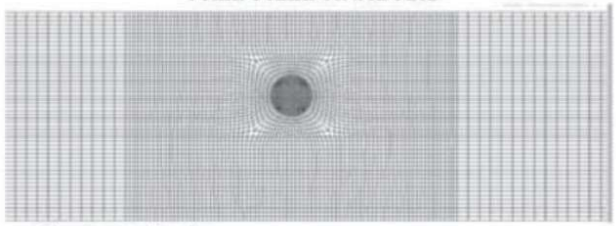

Gravity application

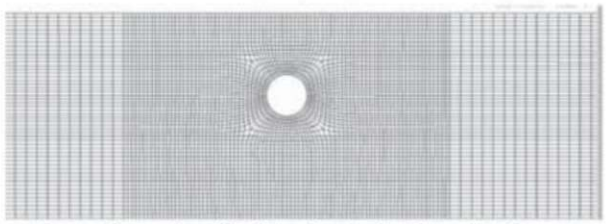

Excavation and application of equivalent boundary forces

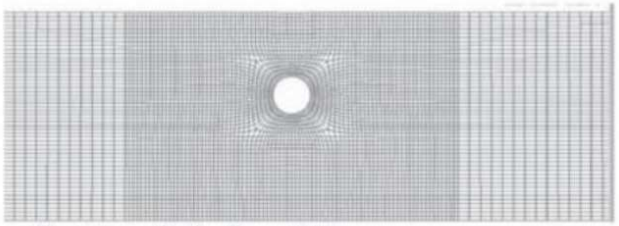

Percentage of unloading = 10%

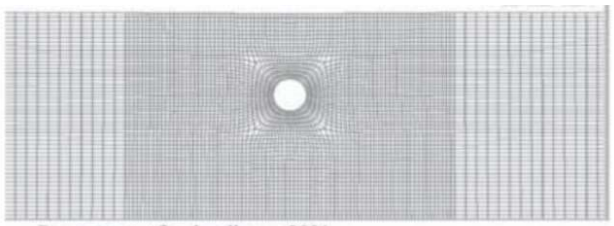

Percentage of unloading = 20%

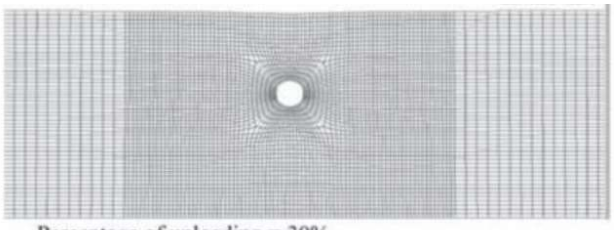

Percentage of unloading = 30%

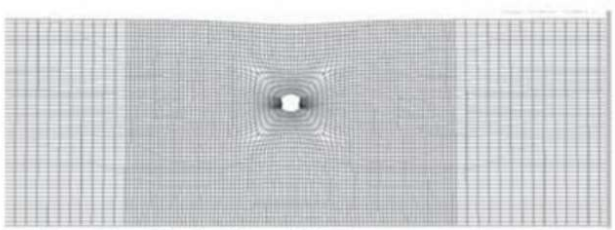

Percentage of unloading = 40%

**Figure 7:** Deformed mesh for different unloading percentages in free field analysis (Amorosi et al., 2012)

#### 4.2.2 Three-Dimensional Methods

Three-dimensional modelling allows the accurate depiction of the induced stress distribution and capture all mechanisms of ground deformations. Certain aspects, like constitutive soil model, tunnel lining, and the construction sequence affect the accuracy of the results. Such aspects are analyzed in more detail in section 5 of this paper. The short-term and long-term behaviour of tunneling can be predicted through coupled soil structure interaction. Current finite element modeling techniques make it possible to model specific details like the face pressure, boundary conditions, the effects of soil improvements either before or during the tunneling process, and other complex ground formations. Hence, this type of 3D numerical modeling is used to predict the actual behaviour of the ground-structure response due to tunneling to provide an inclusive summary of the anticipated structural behaviour, which is essential in designing certain components of a tunnel, like the tunnel shafts.

## 5. Assessment of Modelling Techniques

### 5.1 Nonlinear behavior of Soil

There are several reported constitutive models that can represent the soil behavior. Each model differs in its accuracy. The expected soil behavior, desired accuracy, along with the available data would help in determining the most suitable model to represent a given soil condition. In terms of analytical closed form solutions and numerical simulations (both 2D and 3D), the most notable soil constitutive models are: Linear Elastic Model, Mohr-Coulomb model (MC), The Hardening Soil Model (HS), The Modified Cam-Clay model, and The Soft Soil Model (SS).

The linear elastic material model follows Hooke's law and is based on two parameters: young's modulus and poison's ratio. The displacements obtained through this material model involve heave due to the unloading effects and stress relief, which makes this model unsuitable and unrealistic (Rowe, 1982). This model has been used in many analytical closed-form solutions and numerical simulations.

The Mohr-Coulomb model follows a linear elastic perfectly plastic behavior, where the first part of the model follows a linear elastic response where the strain changes according to a constant young's modulus, adopting a linear loading/unloading behavior. When the stress reaches a certain threshold, presumed failure occurs, and an irreversible plastic strain is developed. This model's behavior is shaped by five material parameters, which are Young's modulus, Poisson's ratio, cohesion, soil friction angle, and dilatancy angle for volume change (Ongsuksun, 2009). Even though this material model has higher accuracy than the linear elastic material model, it is still incapable of realistically modelling soil behavior under such loading conditions. This model has been adopted by various analytical solutions developed to estimate the expected settlement as well as various numerical simulations.

The hardening soil model can reproduce the material performance of different types of soils ranging from stiff to soft soils. This material model utilizes the theory of plasticity rather than elasticity and obtains the failure stress value through the Mohr-Coulomb failure criterion. The behavior of this model is dependent on three different inputted stiffnesses, the triaxial loading stiffness, which allows the computation of elastic and plastic strains, the oedometer stiffness, which considers the plastic strain due to compression, and the triaxial unloading-reloading stiffness, which determines the ground behavior under unloading-reloading conditions (Zakhem and El Naggar, 2019).

The modified cam-clay (MCC) model captures the stress strain behavior of saturated clays. It considers the shear distortion that could occur beneath the state boundary surface. When saturated clays are subjected to stress paths, the rupture is predicted through the Mohr-Coulomb criteria (Roscoe and Burland, 1968). This elastic-plastic strain hardening model utilizes the critical state theory, assuming that the relationship between the mean stress in virgin isotropic compression and the void ratio is logarithmic, and stiffness increases linearly with stress. Mair et al. (1982) modelled the soil conditions using the modified clay model and found that the settlement troughs were wider and flatter than the measured field values. This is attributed to the soil elasticity that dominated the response.

Similarly, the soft soil model is fundamentally based on the modified cam clay model and utilizes the Mohr-Coulomb failure criteria. It is used mainly to model normally consolidated clayey soils that are experiencing primary compression.

### 5.2 Nonlinear behavior of tunnel

The shield tunnel lining is constructed by assembling precast concrete rings bolted together after excavating the desired mass. Each assembled ring has a length of 1-2 m. The TBM machine proceeds to excavate the next compartment of the tunnel bore after each lining ring is effectively erected. Researchers modelled the tunnel lining as a continuous elastic beam or plate. This idealization does not account for the staged construction process and the actual material behavior.

El Naggar et al. (2008) developed a closed-form solution that accounts for the initial stress relief of composite tunnel liners embedded in an infinite elastic medium subject to an initial anisotropic stress field. In this solution, the tunnel lining was idealized as an outer thick-walled cylinder and an inner thin-walled shell. This versatile composite lining solution accounts for several lining geometries and conditions, making it a useful tool for design considerations in tunnelling.

El Naggar and Hinchberger (2006) developed a closed-form solution for slip and non-slip cases considering the lining-ground and lining-lining interfaces. A parametric study compared to the developed closed-form solution with finite element results. The closed-form solution was able to predict the liner’s nonlinear behavior with reasonable accuracy.

Mollon et al. (2013) modelled the concrete lining as perfectly rigid, which is not an accurate depiction of the real conditions. They also assumed perfect contact between the concrete lining and the surrounding soil.

Ngoc-Anh Do et al. (2013) modelled the tunnel as linear elastic linear embedded elements. Such elements model thin liners based on classical Kirchhoff plate theory, where interactions such as the normal directed compressive and tensile interactions and shear directed frictional interactions occur (ICG, 2009; Do et al., 2013). Double node connections were used to simulate the segmented joints between the liner compartments, where the stiffness of the connections was represented by rotational, axial, and radial springs.

Zakhem and El Naggar (2020), modelled the behavior of the concrete tunnel lining using a comprehensive 3D finite element model that accounts for concrete nonlinearity and strain hardening/softening in compression/tension. Interface elements captured the occurrence of slipping, and gapping between the soil and the structure were also used.

### 5.3 Surface settlement

Settlement troughs generally follow a gaussian distribution, where the maximum ground settlement occurs at the center of the curve, usually the tunnel axis. These settlement values range on average from 5 to 13 mm, while the width of the troughs does not exceed 30 meters. Park et al. (2018) performed a case study to estimate the volume loss and settlement troughs through Gaussian fitting, which is based on monitoring and prediction. The volume loss was conducted using a gap model, which considered the geotechnical conditions of the ground and operation conditions. This gap model provided more conservative tail loss predictions.

In numerical analysis, the accuracy of the obtained surface settlement is predominantly affected by the used constitutive soil model. Advanced nonlinear strain hardening models were more accurate, as compared to other constitutive models when predicting the surface settlement resulting from tunneling. The overall surface settlement was found to increase due to the passage of the shield body and while injecting the gap between tail skin and concrete lining with grout.

A significant increase in settlement occurs until the dissipation of most of the excess pore water pressure (Zakhem and El Naggar, 2020). Such settlement increases are due to the tunnel penetrating through highly nonlinear soils. Hence, constitutive soil models able to account for high soil stiffness at very small strains is essential to obtain accurate results (Zakhem and El Naggar 2020; Moller & Vermeer, 2008; Hejazi et al., 2008; Addenbrooke et al., 1997). Hardening soil models were able to predict the soil performance with higher accuracy due to accounting for the complicated soil behavior including densification, stress-dependent stiffness, pre-consolidation, dilatancy, and plastic strains at yielding.

### 5.4 Earth pressure on tunnel lining

Depending on the geometric and geologic conditions of a given tunnel, linings are usually designed to support a certain portion of the overburden pressure (Terzagh, 1943). Even though full contact between the lining and supporting soil is assumed when calculating the possible lining loads, local support loss may develop around the tunnel, due to improper grouting, erosion of supporting soils, and many other reasons. Voids eventually initiate around the tunnel linings through weakened zones caused by the inflow of groundwater carrying fines through the existing cracks (Asakura and Kojima, 2003). This resulting contact loss causes a redistribution of the earth pressure acting on the lining, thereby changing the internal forces in the lining structure (Leung and Meguid, 2011).

The accuracy of numerically evaluated earth pressure distributions depends on the adopted consecutive soil model. To evaluate the accuracy of each constitutive soil model, Zakhem and El Naggar (2019) compared the different results obtained from utilizing the hardening soil model (HS), hardening soil model with small strain stiffness (HSS), the modified cam-clay model (MCC), and the soft soil model (SS) against field measurements by Lee et al. (1999) at the five locations shown in Figure 8. Figure 9 shows a decrease in earth pressure occurring gradually with time, primarily due to the consolidation effect of the grouting material.

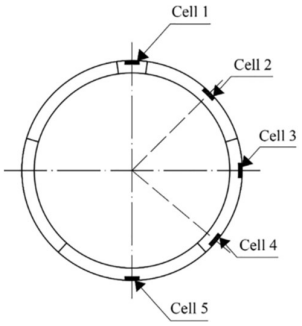


**Figure 8:** Layout of earth pressure cells

### 5.5 Construction sequence

Idealizing and simulating the correct construction sequence for a tunneling project affects the accuracy of the simulation results. Ngoc-Anh Do et al. (2013) developed a model through FLAC 3D modelling software, based on the finite difference method, using small strain calculations. He followed a step by step approach, where each excavation step corresponded to an advancement of the tunnel face, equal to the width of the lining ring. The step excavation modelling technique is followed by many other researchers, due to its effectiveness in capturing the overall behavior of the construction process.

Mollon et al. (2013) followed a step by step excavation process, where each step was 1 m long. This simulation contained 35 steps and allowed obtaining the instantaneous settlements at the last 1 m of the excavation process. An imbalance is created between the earth pressure inside the TBM soil chamber, the earth, and the hydrostatic pressure that exists past the cutter disk chamber within the TBM compartments. To eliminate this

imbalance, grouting material is infused between tunnel lining and the tail skin. Mollon et al. (2013) modelled this grouting action in two phases; a liquid phase represented by a pressure acting on the ground surface and tunnel lining, and a solid state.

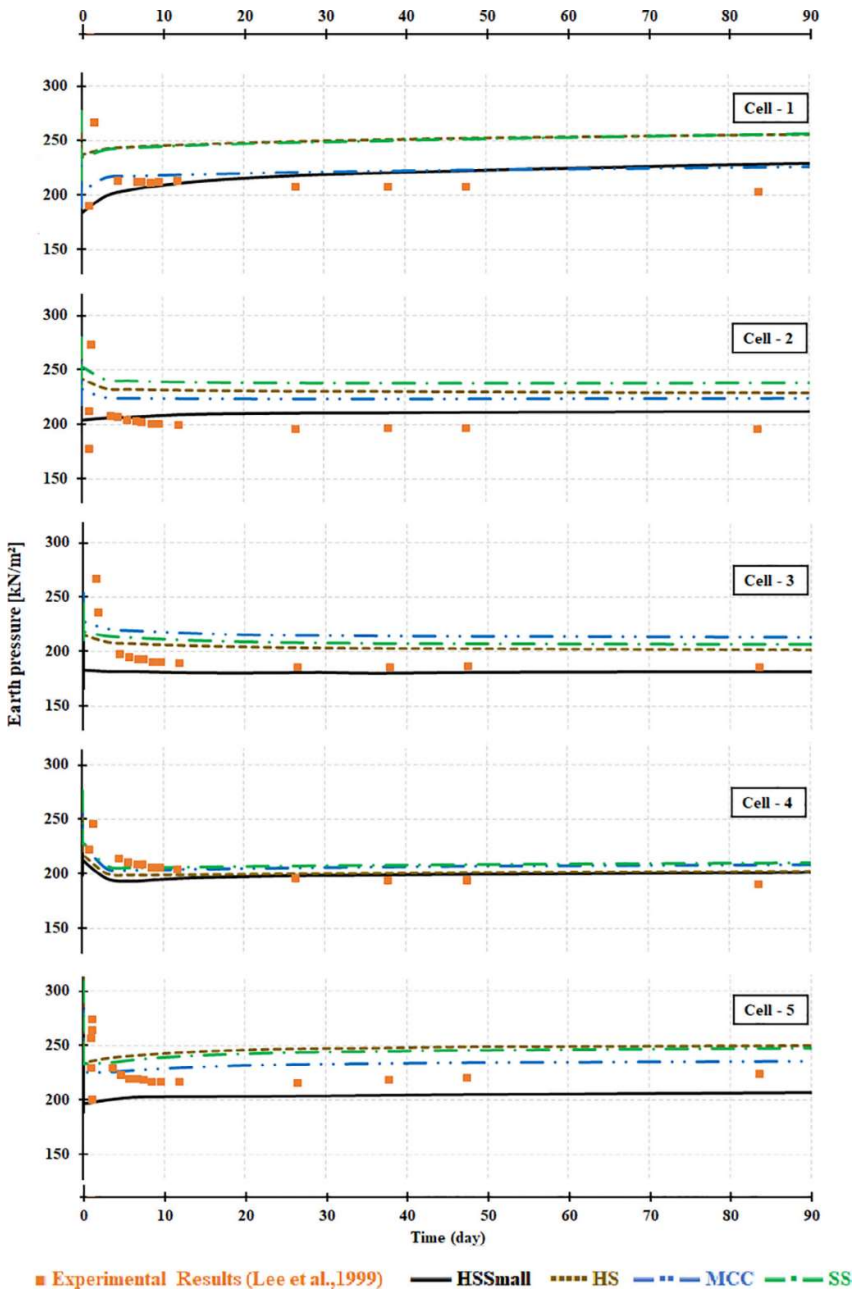


**Figure 9:** Comparison of the development of earth pressure around the tunnel lining.

Zakhem and Elnaggar (2019) developed a sophisticated model of the EPB shield tunnelling process. The installation of each ring was divided into repetitive excavation steps. In the first step, the soil in front of the EPB shield got excavated and the support pressure was applied at the tunnel face to maintain balance. The tunnel face pressure was a bentonite pressure that linearly increased with depth. The EPB shield was then activated and the conicity of the shield was modelled in the numerical simulation. The lining segments developed using volume elements were installed consecutively in circumferential direction forming a ring (developed from 6 segments). Interface elements allowed rotation and shear transfer between the segments. Backfill grout pressure at the back of the EPB shield was modelled, where the grout was modelled using the concrete model in PLAXIS 3D, and the applied grout pressure decreased with distance to simulate the fresh grout hardening and stiffening with time. The steps involved in this numerical simulation are summarized in Figure 10.

One of the most sophisticated and complex construction sequences was modelled via a step by step technique by Zakhem and El Naggar (2020), which was modelled through PLAXIS. Each construction advancement was divided into six steps. The first step in each advancement was the face excavation, where the mass is excavated, water conditions dry, and surface construction activated. Face pressure is simulated in this step. In the second step, the TBM shield's conical compartment is defined, and thus, the face pressure gets deactivated. In steps # 3 and 4, the shield has a constant diameter, so the outer surface contraction is set to uniform. The grout injection procedure is modelled in step 5 of the idealized construction procedure. In step 6, the fresh grout introduced in step 5 is set to dry. Linear elastic models simulated this effect, where fresh grout had a modulus of elasticity of 2 GPa and hardened grout had a modulus of elasticity of 10 GPa. Finally, in step 7 the grout hardens, and the excavation proceeds to the next ring. This complex realistic modelling approach directly enhanced the accuracy of the simulation's results.

## 6. Conclusions

The need to anticipate the effects tunnel construction would have on preexisting structures, and the soil structure interaction resulting from such activity cannot be underestimated. Understanding such interactions would allow urban planners and engineers to avoid any possible design oversight or failure catastrophes. This paper presents a thorough evaluation of the different techniques for assessing the effects tunneling on surrounding structures, including techniques that capture both coupled and uncoupled soil structure interaction methods. It provides the basis for geotechnical engineers to gain understanding in this critical area of tunneling.

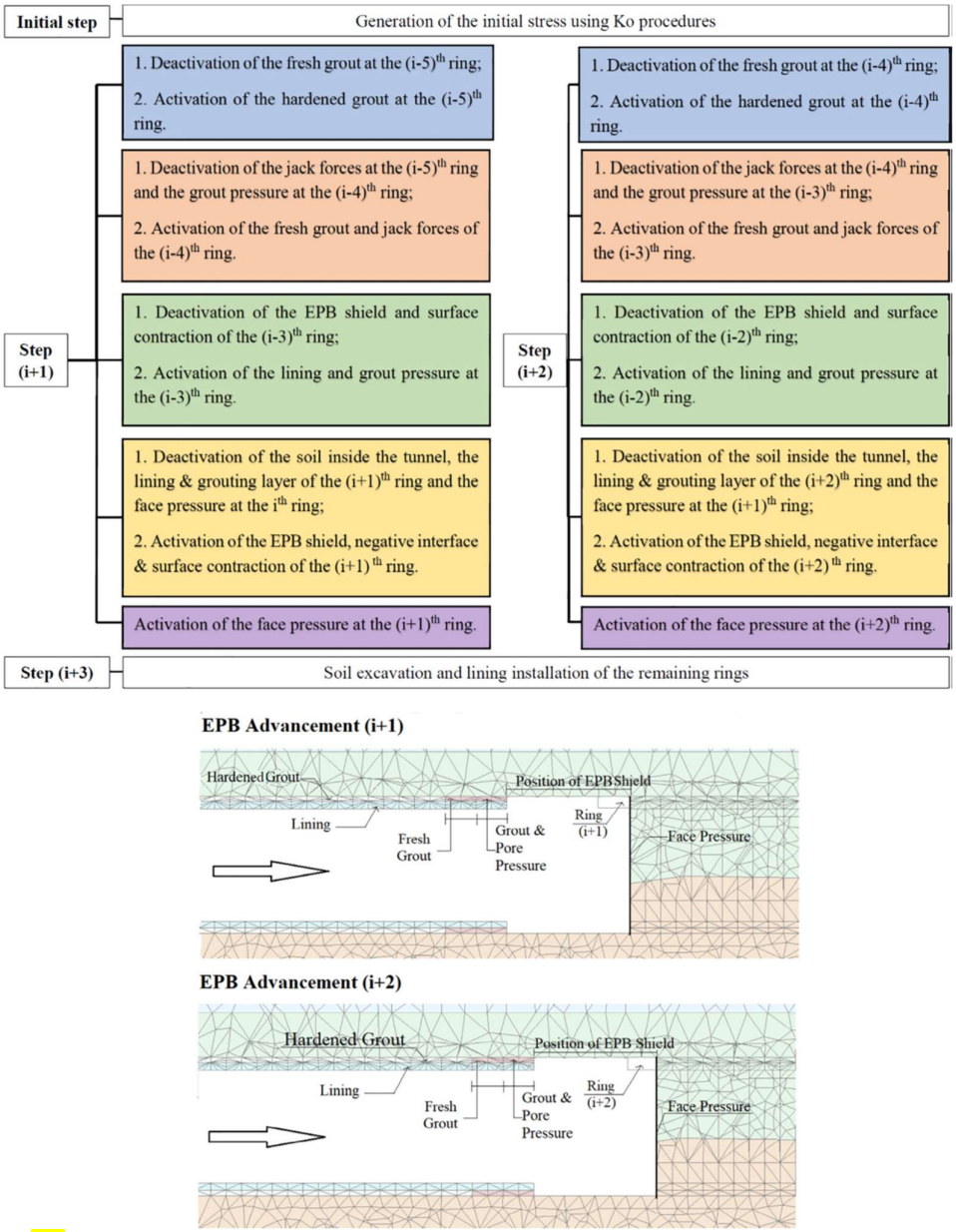


**Figure 10:** Steps involved in Zakhem and El Naggar (2019)'s numerical simulation

## 7. Acknowledgement

The authors are grateful for the financial support provided by the Natural Sciences and Engineering Research Council of Canada (NSERC).

## 8. References


Abdel-Meguid M, Rowe RK, Lo KY. (2002). 3D effects of surface construction over existing subway tunnels. Int J Geomech;2(4):447–69.

Addenbrooke T, Potts D, Puzrin A. (1997). The influence of prefailure soil stiffness on the numerical analysis of tunnel construction. Geotechnique; 47(3):693–712.

Al-Omari1a, R. R., Al-Azzawi, A. A., & AlAbbas, K. A. (2016). Behavior of piled rafts overlying a tunnel in sandy soil.

Asakura, T., & Kojima, Y. (2003). Tunnel maintenance in Japan. Tunnelling and Underground Space Technology, 18(2-3), 161-169.

Atkinson, J. H., Orr, T. L. L., and Potts, D. M. (1975). Research studies into the behaviour of tunnels and tunnel linings in soft ground. TRRL, supp report 176

Amorosi, A., Boldini, D., de Felice, G., & Malena, M. (2012). Tunnelling-induced deformation on a masonry structure: A numerical approach: A. Amorosi D. Boldini. In *Geotechnical Aspects of Underground Construction in Soft Ground* (pp. 371-378). CRC Press.

Bobet, A. (2001). ‘‘Liner stresses in tunnels in saturated ground.’’Internal Rep., Purdue University, West Lafayette, Ind.

Bobet, A. (2001). Analytical Solutions for Shallow Tunnels in Saturated Ground. *Journal of Engineering Mechanics*, *127*(12), 1258–1266. https://doi.org/10.1061/(ASCE)0733-9399(2001)127:12(1258)

Bouvard, M., and Pinto, N. (1969). ‘‘Ame´nagement Capivari-Cachoeira: E´tude du puits en charge.’’ La Houille Blanche, Paris, 7, 747–760.

Briggs, H. (1929). Mining Subsidence, London, Arnold, 215.

Davis, E. H., et al. (1980). The stability of shallow tunnels and underground openings in cohesive material. Geotechnique, 397-416

De Melo GP, Pereira SC. Three-dimensional numerical modelling of the construction of an EPBS tunnel for Shanghai Metro - Line 2. Geotech Aspects Undergr Construct Soft Ground 2002:323–8.

Do, N. A., Dias, D., Oreste, P. P., & Djeran-Maigre, I. (2013). 3D modelling for mechanized tunnelling in soft ground-Influence of the constitutive model. *American Journal of Applied Sciences*, 10(8), 863-875.

Do, N.A., D. Dias, P. Oreste and I. Djeran-Maigre. (2013). 2D numerical investigation of segmental tunnel lining behavior. Tunnell. Underground Space Technol., 37: 115-127. DOI: 10.1016/j.tust.2013.03.008

Einstein, H. H., and Schwartz, C. W. (1979). ‘‘Simplified analysis for tunnel supports.’’ J. Geotech. Engrg. Div., ASCE, 105(4), 499–518.

El Naggar, H., & Hinchberger, S. (2008b). An analytical solution for jointed tunnel linings in elastic soil or rock. *Canadian Geotechnical Journal*, *45*(11), 1572–1593. https://doi.org/10.1139/T08-075

El Naggar, H., Hinchberger, S. D., & El Naggar, M. H. (2008). Simplified analysis of seismic in-plane stresses in composite and jointed tunnel linings. *Soil Dynamics and Earthquake Engineering*, *28*(12), 1063-1077.

El Naggar, H., Hinchberger, S., & Lo, K. (2008a). A closed-form solution for composite tunnel linings in a homogeneous infinite isotropic elastic medium. *Canadian Geotechnical Journal*, *45*(2), 266–287. https://doi.org/10.1139/T07-055

El Naggar, Hany H. (2007). Analysis and Evaluation of Segmental Concrete Tunnel Linings - Seismic and Durability Considerations. The University of Western Ontario, London, Ontario.
Ellis, D., & Glover, B. (2019). 2019 URBAN MOBILITY REPORT.
Ferna´ndez, G., Tirso, A., and Alvarez, A., Jr. (1994). ‘‘Seepage-induced effective stresses and water pressures around pressure tunnels.’’ J. Geotech. Engrg., ASCE, 120(1), 108–128.
Fang, Y. S., Lin, J. S., & Su, C. S. (1994). An estimation of ground settlement due to shield tunnelling by the Peck–Fujita method. *Canadian geotechnical journal*, *31*(3), 431-443.
Fujita, K. (1982). Prediction of surface settlements caused by shield tunnelling. Iiz Proceedings, International Conference on Soil Mechanics, Mexico City, Vol. 1. pp. 239-246.
Fujita, K., and Ueda, K. (1978). Predicted and observed movement of surroundings during construction of underground structures. Irz Proceedings, Seminar on Tunnels and Underground Structure Technology, Chinese Institute of Civil and Hydraulic Engineering, Taipei, Taiwan, June 12-14, 1978. pp. 133-163
Goldreich, A.H., 1913, Die Theorie der Bodensenkungen in Kohlengebieten, Berlin.
Glossop, N.H., and O'Reilly, M.P. 1982. Settlement caused by tunnelling through soft marine silty clay. Tunnels and Tunnelling, 14(9): 13-16.
Hardin BO, Drnevich V. (1972). Shear modulus and damping in soils: design equations and curves. Geotech Special, 98(118).
Hejazi Y, Dias D, Kastner R. (2008). Impact of constitutive models on the numerical analysis of underground constructions. Acta Geotech; 3(4):251–8.
ICG, 2009. FLAC Fast Lagrangian Analysis of Continua, Version 4.0. User’s Manual.
Karakus M (2006) Appraising the methods accounting for 3D tunneling effects in 2D plain strain FE analysis. Tunn Undergr Sp Technol 22:47–56.
Khabbaz, H., Gibson, R., & Fatahi, B. (2019). Effect of constructing twin tunnels under a building supported by pile foundations in the Sydney central business district. *Underground Space*, *4*(4), 261-276.
Kimura, I, and Mair, R. J. (1981). Centrifugal testing of model tunnels in soft clay. (Proceedings of the 10th International Conference on Soil Mechanics and Foundation Engineering, Stockholm, vol.1, 319-22
Lee K, Ji H, Shen C, Liu J, Bai T. Ground response to the construction of Shanghai metro tunnel-line 2. Soils Found 1999;39(3):113–34.
Leung, C., & Meguid, M. A. (2011). An experimental study of the effect of local contact loss on the earth pressure distribution on existing tunnel linings. *Tunnelling and underground space technology*, *26*(1), 139-145.
Liu, H., Liao, X., Zhang, J., Li, N., Yu, Z., & Yao, Q. (2011). Numerical analysis of bearing capacity of pile foundation due to urban metro tunneling. In *Contemporary Topics on Testing, Modeling, and Case Studies of Geomaterials, Pavements, and Tunnels* (pp. 191-197).
Lo, K. Y., & Yuen, C. M. (1981). Design of tunnel lining in rock for long term time effects. *Canadian Geotechnical Journal*, *18*(1), 24-39.
Loganathan, N., & Poulos, H. (1998). Analytical Prediction for Tunneling-Induced Ground Movements in Clays. *Journal of Geotechnical and Geoenvironmental Engineering*, *124*(9), 846–856. https://doi.org/10.1061/(ASCE)1090-0241(1998)124:9(846)
Mandel, G., and H. Wagner. (1968). Verkehrs-Tunnelbau, Band I, Planning, Entwurf und Bauausfuhrung, W. Ernst u. Sohn, Berlin-Munchen, Germany
Mair R, Gunn M, O'Reilly M. (1982). Ground movements around shallow tunnels in soft clay. Tunnels Tunnel.

Mair, R. J. (1979). Centrifugal modelling of tunnel construction in soft clay. Cambridge University. *Ph.D thesis*.

Mair, R. J., Gunn M. J., and O'Reilly, M. P., Ground movements around shallow tunnels in soft clay, 323-8

Martos, F. (1958). Concerning an approximate equation of the subsidence trough and its time factors. International Strata Control Congress, Leipzig 191-205

Matsumoto, Y., and Nishioka, T. (1991). Theoretical tunnel mechanics, University of Tokyo Press, Tokyo.

Moller S, Vermeer P. (2008). On numerical simulation of tunnel installation. Tunn Undergr Sp Technol;23(4):461–75.

Mollon, G., Dias, D., & Soubra, A. (2013). Probabilistic analyses of tunneling-induced ground movements. *Acta Geotechnica, 8*(2), 181-199.

Morgan, H.D. (1961). A contribution to the analysis of stress in a circular tunnel. Ge´otechnique, 11: 37–46.

Muir Wood, A.M. (1975). The circular tunnel in elastic ground. Ge´otechnique, 25: 115–127.

Namazi, E., & Mohamad, H. (2013). Assessment of building damage induced by three-dimensional ground movements. *Journal of geotechnical and geoenvironmental engineering*, *139*(4), 608-618.

Negro, A., & De Queiroz, P. I. B. (2000). Prediction and performance: a review of numerical analyses for tunnels. *Geotechnical aspects of underground construction in soft ground*, 409-418.

Netzel, H. (2004). Empirical, Analytical Methods for Surface Settlement Prediction Due to TBM-Tunnelling in Dutch Soft Soil.

O'Reilly, M., & New, B. (2015). SETTLEMENTS ABOVE TUNNELS IN THE UNITED KINGDOM - THEIR MAGNITUDE AND PREDICTION. *Tunnels & Tunnelling International*, 56–66,5. Retrieved from http://search.proquest.com/docview/1682903684/

Ongsuksun, B., Sture, S., Ko, H., McCartney, J., & Walter, H. (2009). *Three-dimensional analysis of displacements resulting from tunneling in soft ground* (ProQuest Dissertations Publishing). Retrieved from http://search.proquest.com/docview/304867448/

Papanikolaou, V. K., & Kappos, A. J. (2014). Practical nonlinear analysis of unreinforced concrete tunnel linings. *Tunnelling and underground space technology*, *40*, 127-140.

Park, H., Oh, J. Y., Kim, D., & Chang, S. (2018). Monitoring and Analysis of Ground Settlement Induced by Tunnelling with Slurry Pressure-Balanced Tunnel Boring Machine. *Advances in Civil Engineering*, *2018*.

Peck, R. B. (1969). Deep Excavation and Tunneling in Soft Ground, General Report, Session 4, 7th Int. Conf. SM and FE, Mexico City

Rankine, R.E., Ghaboussi, J., and Hendron, A.J. (1978). Analysis of ground-liner interaction for tunnels. Report No. UMTA-IL-06– 0043–78–3, Department of Civil Engineering, University of Illinois at Urbana Champaign, p. 441.

Roscoe K, Burland J.(1968). On the generalized stress-strain behavior of wet clays. In: Heyman J, Leckie F, editors. Engineering plasticity. Cambridge: Cambridge University Press. p. 535–609.

Rowe, R. K., and Kack, G. J. (1983). "A theoretical examination of the settlements induced by tunnelling: Four case histories." Can. Geotech. J., Ottawa, Canada, 20, 299-314.

Schadlich B, Schweiger H. (2014). Shotcrete model. Internal report: Implementation, validation and application of the shotcrete model. Computational Geotechnics Group, Institute for Soil Mechanics and Foundation Engineering, Graz University of technology.

Schmidt, B. (1969). Settlements and ground movements associated with tunnelling in soil. *PhD Thesis*.

T. Asakura, Y. Kojima, 2003.Tunnel maintenance in Japan. Tunnelling and Underground Space Technology, 18 (2003), pp. 161-169

Terzaghi, K.N., 1943. Theoretical Soil Mechanics, Wiley, New York.

Terzaghi, K. (1942). Shield Tunnels of the Chicago Subway, J. Boston Soc. Civ. Engr., V.29, 163-210

Verruijt, A., & Booker, J. R. (1998). Surface settlements due to deformation of a tunnel in an elastic half plane. *Geotechnique*, *48*(5), 709-713.

Vlachopoulos, N., & Diederichs, M. S. (2014). Appropriate uses and practical limitations of 2D numerical analysis of tunnels and tunnel support response. *Geotechnical and Geological Engineering*, *32*(2), 469-488.

Yildizlar, B., Sayin, B., Karakas, A. S., & Akcay, C. (2014). Structural damage caused to RC buildings by tunnelling work.

Yuen, C.M. 1979. Rock-Structure time interaction. Ph.D. thesis, Department of Civil and Environmental Engineering. The University of Western Ontario, London, Ontario.

Zakhem, A. M., & El Naggar, H. (2016). STR-949: DISTURBANCE TO NEARBY SURFACE STRUCTURES CAUSED BY TUNNELING INDUCED GROUND DISPLACEMENTS.

Zakhem, A. M., & El Naggar, H. (2019). Effect of the constitutive material model employed on predictions of the behaviour of earth pressure balance (EPB) shield-driven tunnels. *Transportation Geotechnics*, *21*, 100264.

Zakhem, A. M., & El Naggar, H. (2020). Three-dimensional investigation of how newly constructed buildings supported on raft foundations affect pre-existing tunnels. *Transportation Geotechnics*, *22*, 100324.

Zhang, D., Fang, Q., Hou, Y., Li, P., & Yuen Wong, L. N. (2013). Protection of buildings against damages as a result of adjacent large-span tunneling in shallowly buried soft ground. *Journal of geotechnical and geoenvironmental engineering*, *139*(6), 903-913.'